

Evolution of Nanoscale Pore Structure in Coordination Polymers During Thermal and Chemical Exposure Revealed by Positron Annihilation

By Ming Liu, Antek G. Wong-Foy, Richard S. Vallery, William E. Frieze, Jennifer K. Schnobrich, David W. Gidley,* and Adam J. Matzger*

Over the past decade, nanostructured materials constructed from metal ions/clusters linked by organic groups were demonstrated to have remarkably high porosity and specific surface areas higher than the best activated carbons.^[1–5] These microporous coordination polymers (MCPs), are self-assembled, periodic, porous structures that have redefined what is possible with adsorption.^[6–9] Hydrogen storage and CO₂ sequestration are two of the most intensively studied areas with record-setting capacities achieved for several MCPs.^[10–12] Despite these performance advantages, MCPs suffer from an incomplete understanding of the fundamental mechanisms of adsorption; furthermore problems with structural integrity and poor atmospheric/temperature stability are compounded by difficulties in characterizing structural damage. Although X-ray diffraction and gas-adsorption techniques have facilitated the development of MCPs, these methods give a structurally averaged picture of the pore structure and are therefore ill-suited to study defects and other nonperiodic phenomena of critical importance for future applications. In particular, their value for monitoring pore structure evolution under conditions directly relevant for sorption applications is limited. Positronium annihilation lifetime spectroscopy (PALS) is an in situ pore-/void-volume characterization technique,^[13] in which the shortening of the annihilation lifetime of Ps (Ps = positronium, the hydrogenlike bound state of an electron with its antiparticle, the positron) due to collisions with the pore walls is correlated with the pore size. Ps readily forms by electron capture when positrons are injected into insulators. Moreover, it is energetically favorable for Ps to localize inside voids providing a natural probe from within. The Ps lifetime is correlated with pore size^[14–17] and the relative intensity of this component is related to the porosity of the material. In this first application of PALS to MCPs we demonstrate its unique ability to

uncover new phenomena in these materials with nanoscale porosity.

MOF-5^[18] (MOF = metal–organic framework) is one of the earliest examples of an exceptionally high surface area MCP and the most thoroughly investigated representative of this class. Therefore, it is an ideal benchmark to test the suitability of PALS and presents an extremely challenging system, in which to reveal new phenomena. The material is an open cubic structure that consists of face-sharing cubic cages that extend in all three dimensions (see Fig. S1 in the Supporting Information). A high-quality sample ($\sim 1\text{ cm}^3$) of MOF-5 crystals ($\sim 0.5\text{-mm}$ cubic crystals) with a Brunauer–Emmett–Teller theory (BET) surface area of $3500\text{ m}^2\text{ g}^{-1}$ was prepared for the PALS experiments. Ps, formed via electron capture by a positron in this MCP framework, is energetically driven into the pores. Fitting of the PALS time spectrum (a typical spectrum is Fig. S2 in the Supporting Information) reveals, surprisingly in the light of the supposedly uniform pores in MOF-5, two Ps lifetimes: a 13 ns component corresponding to $\sim 85\%$ of the total Ps formed and an 86 ns component representing the remaining 15%. The reduction in the lifetime of Ps from 142 ns in vacuum due to additional annihilation with electrons in the pore walls is directly calibrated to the pore size using the Tao–Eldrup model^[14,15] and recent extensions.^[16,17] The short-lifetime component, corresponding to a 1.5 nm cubical pore, is unequivocally that of Ps probing the MOF-5 framework and is the principle focus of this work. The long lifetime is attributed to open-volume defects in the crystal with a characteristic size of $\sim 6\text{ nm}$: this unexpected length scale of defects has not been observed in MOF-5 and we will return to this indicator of long-range disorder later in this paper.

We now consider how Ps is confined by and interacts with the framework of MOF-5. The measured temperature dependence of the $\sim 13\text{ ns}$ framework lifetime (Fig. 1) provides information on the nature of Ps confinement. The thermally excited states of Ps in a pore have progressively more overlap with pore walls at higher temperature and, hence, faster Ps annihilation rates result in shortened lifetimes (see the Supporting Information). The results in Figure 1 indicate that Ps in the framework is not localized in three dimensions as it would be the case if Ps was trapped in a cubical cage (see the Supporting Information for more details). The better agreement with a 2D confined model suggests that Ps is mobile along an axis of long rectangular pores of a square (2D) cross section, 1.25 nm on a side. This implied mobility of Ps within the framework can be quantified with a PALS spectrometer implemented on a low-energy focused beam

[*] Prof. A. J. Matzger, Dr. A. G. Wong-Foy, J. K. Schnobrich
Department of Chemistry, University of Michigan
930 N. University St., Ann Arbor, MI 48109 (USA)
E-mail: matzger@umich.edu

Prof. D. W. Gidley, Dr. M. Liu, Dr. W. E. Frieze
Department of Physics, University of Michigan
450 Church St. Ann Arbor, MI 48109 (USA)
E-mail: gidley@umich.edu

Prof. R. S. Vallery
Department of Physics, Grand Valley State University
151 Padnos Hall, Allendale, MI 49401 (USA)

DOI: 10.1002/adma.200903618

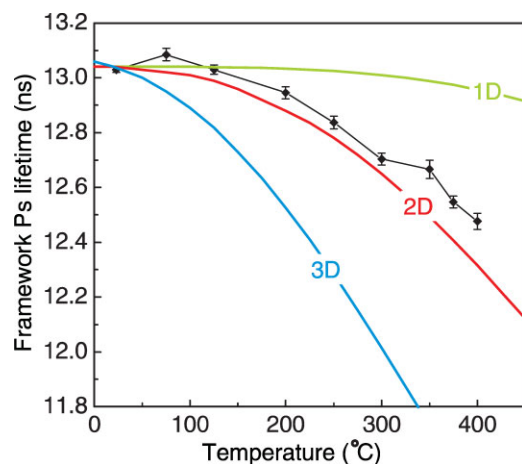


Figure 1. Determining Ps mobility within the MOF-5 framework. Fitted Ps lifetime in the framework at elevated temperatures compared to predictions of the 1, 2, and 3-dimensionally confined extended Tao–Eldrup pore models. These fully reversible and reproducible results (up to 400 °C) are consistent with a simple model of Ps confined to long channels, where it is free to move along the channel axis.

of positrons that permits controlled, shallow implantation of positrons/Ps below the crystal surface (see the Supporting Information for more details). With this technique a Ps diffusion length within the MOF-5 framework of approximately 2 μm (roughly 1500 cages) is deduced.

Hence, Ps is confirmed to be free to diffuse through the vacant framework during its 13 ns lifetime and sample many thousands of cells. For comparison, measurements were made on a zinc 2-methylimidazole MCP^[19] and a positron lifetime of 7.4 ns, corresponding to Ps trapped in a spherical pore of 1.15-nm diameter (effective diameter from crystallography = 1.25 nm), was fitted; in contrast to MOF-5, essentially no Ps escape into vacuum is detected, signaling slow kinetics of Ps diffusion. Therefore, it can be concluded that kinetics of diffusion can vary widely between MCPs: a likely result of differences in pore aperture and geometry.

Beyond providing new information on the evacuated framework in MCPs, PALS has a unique ability to offer in situ porosity information during adsorption, chemical attack, and thermally induced damage. To demonstrate the sensitivity of PALS to the presence of adsorbate, the framework lifetime of Ps is shown versus CO₂ pressure in Figure 2a. The decreasing lifetime as pressure increases provides a direct measure of vacant pore-size diminution as the framework thickens by CO₂ adsorption. After conversion to pore size using either a long-channel (2D) or cubical (3D) pore model^[16,20] we can calculate the fractional occupation (filling) of the original cell, as shown in Figure 2b. Consistent with traditional adsorption measurements the volume occupied (hence the mass absorbed) by “liquidlike” CO₂ asymptotically levels off over 200 psi.^[21] Remarkably, PALS reveals that there is still unfilled porosity even at 400 psi—the framework Ps lifetime approaches 4 ns, not zero, corresponding to a cubical pore of 0.8 nm side-length, i.e., some 20–30% of the open volume is still unfilled by CO₂ at saturation. This indicates that simple pore filling in MOF-5 is not operative and either monolayer or multilayer adsorption occurs. This result uniquely

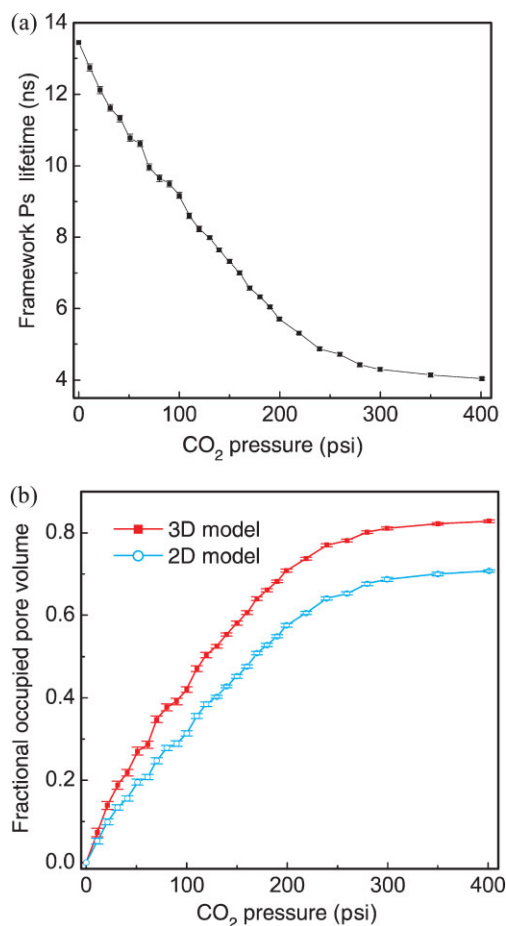


Figure 2. CO₂ adsorption into MOF-5. a) The framework Ps lifetime as a function of CO₂ pressure. Despite the strong decrease in lifetime, the relative intensity of Ps in the framework was constant with pressure. b) The calculated volume fraction of the MOF-5 cage occupied by CO₂ as a function of CO₂ pressure assuming either a 3D cubic pore model or a 2D square channel model.

provides a picture of how much space could be exploited in the material for additional gas-storage capacity, thus aiding new sorbent designs or choice of chemical impregnants.^[1,22–25] For example, the prediction is that a MOF-5 analog with an additional 0.8-nm adsorption site in the center of the pore would not negatively impact CO₂ uptake. It would, however, add an additional attractive potential that would lead to higher affinity, thus achieving saturation at lower pressures.

Returning to the issue of the long-lifetime Ps component (corresponding to defects) initially observed in the PALS spectrum of MOF-5 under vacuum, its lifetime and intensity are also affected by CO₂ adsorption. The fact that PALS reveals these defects in the MOF-5 structure is particularly significant because neither nitrogen adsorption nor X-ray diffraction detect these features. Figure 3a shows the fitted defect Ps lifetime versus CO₂ pressure and Figure 3b shows the corresponding relative Ps intensity. The red curve in Figure 3a is a completely independent measurement of Ps lifetimes in pure CO₂ gas, reported in 1983.^[26] The near-perfect agreement in the lifetime data at high pressure indicates that above 200 psi Ps is predominantly

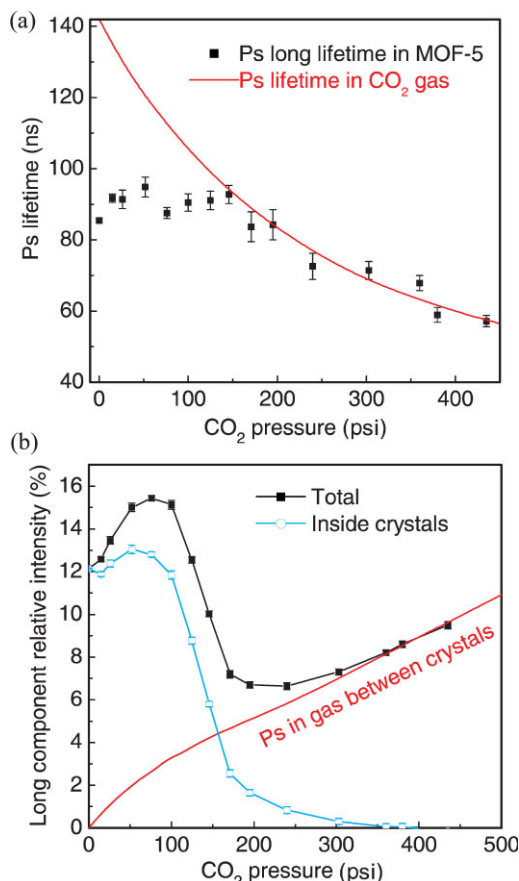


Figure 3. The evolution of the long-lived (defect) Ps component of MOF-5 versus CO₂ pressure. a) The Ps lifetimes and b) the corresponding relative intensities. This Ps component evidently has two origins in MOF-5: Ps annihilating in 6-nm defects with intensities plotted in (b) with open symbols (the result of subtracting the smooth curve from the total intensities) and Ps formed and annihilating in the CO₂ gas surrounding the crystal grains.

annihilating in the gas between the crystals without interaction with the MCP. The red curve in Figure 3b is an estimate of the contribution of such Ps formation in the gas to the total. The deviation of the data from the red lines at low gas pressure indicates the existence of a distinct population of Ps formed *within* the MCP and annihilating in defects that are so large that CO₂ adsorption has minimal effect on their size. The lifetime of this Ps component at low pressures is 86 ns corresponding to defects ~6 nm in size. The intensity of Ps annihilating in these 6-nm defects (blue curve in Fig. 3b) is nearly constant up to 100 psi but then drops sharply between 100 and 200 psi. The disappearance of this Ps population as the pressure rises above ~200 psi indicates that the primary mechanism for Ps populating these defects in MOF-5 is Ps diffusion through the framework and this mobility is curtailed by CO₂ blockage of framework diffusion paths. In fact, the mass loading at which this blockage occurs gives a quantitative measure of when guest presence controls the kinetics of diffusion through the framework: a critical issue in kinetically limited separations with MCPs.

In order to determine the volume fraction (porosity) contributed by these 6-nm defects, an N₂-adsorption experiment

was performed revealing clean type-I behavior. The isotherm of this null result can only set an upper limit of ~1% on any porosity in such large defects in MOF-5. PALS can offer a quantitative estimate based on the beam result (Ps diffusion length = 2 μm) and bulk result (15% of all Ps can diffuse into and trap in the 6-nm defects). Since Ps is formed uniformly throughout the framework it can be concluded that 15% of the crystal volume of MOF-5 must be located within the 2 μm Ps diffusion length of these defects. Assuming the defects to be planar cracks, a ~27 μm spacing between cracks is deduced. The contribution to the porosity of 6-nm-wide cracks every 27 μm would only be about 0.02%, thus, rendering them virtually impossible to detect with traditional gas adsorption techniques. This defect detection technique is applicable to any MCP for which Ps is mobile within the framework and the sensitivity for detection will be related to how long the Ps diffusion length is.

To explore the capabilities of PALS to probe the evolution of framework damage the in situ heating experiment (Fig. 1a) was extended above 400 °C. At 420 °C the first evolution of gas from the sample is detected (consistent with that observed in thermogravimetric analysis)^[18] and irreversible change occurs in PALS (Fig. 4a): the framework lifetime begins to deviate from that initially observed in Figure 1a and, after 3 h, adequate fitting of the lifetime spectrum requires at least a second Ps lifetime around 7 ns that decreases with exposure time and temperature. This changing of the second lifetime suggests that progressive framework collapse is producing a range of voids smaller than the framework size. The total Ps intensity (Fig. 4b) is concomitantly decreasing, mainly attributable to the sharp drop in intensity of the ~12-ns framework lifetime. After 5 h at 420 °C the sample was allowed to cool to 23 °C and a high-statistics 15 h run was acquired. Using PALS continuum lifetime fitting methods^[27] we fit a pore size distribution (PSD) in Figure 4c that more clearly shows thermally induced framework degradation. The PSD of the undamaged MOF-5 is consistent with a sharp peak—i.e., all Ps in the framework samples the same average environment and, hence, decays with a single Ps lifetime/mean pore size. Thermal degradation produces an increasingly broad range of Ps lifetimes (pore sizes) indicating that locally the damage is severe enough to form regions of smaller, partially collapsed pores that now trap Ps, thus curtailing its diffusion. The necessity for fitting at least two framework Ps lifetimes in Figure 4a is simply a way for discrete lifetime fitting to approximate a PALS spectrum that is actually a continuum of Ps lifetimes. Consistent with reduced Ps diffusion length the intensity of Ps annihilating in the 6-nm defects monotonically drops by more than a factor of two. Cycling to room temperature was repeated after heating at 420 °C for additional 5 h, 440 °C for 7 h, and 460 °C for 3 h. The fraction of Ps annihilating in partially collapsed pores grows as damage accumulates. However, the total intensity of Ps annihilation in Figure 4b has decreased by a factor of five indicating severe loss of porosity in these nanometer voids. Consistent with this, post-treatment nitrogen sorption analysis reveals a loss in specific surface area from 3500 m² g⁻¹ to 924 m² g⁻¹. The results in Figure 4 provide unprecedented snapshots of thermally induced pore degradation from the onset of well-separated localized damage to widespread damage of the framework with extensive disappearance of microporosity accompanied by smaller-pore formation.

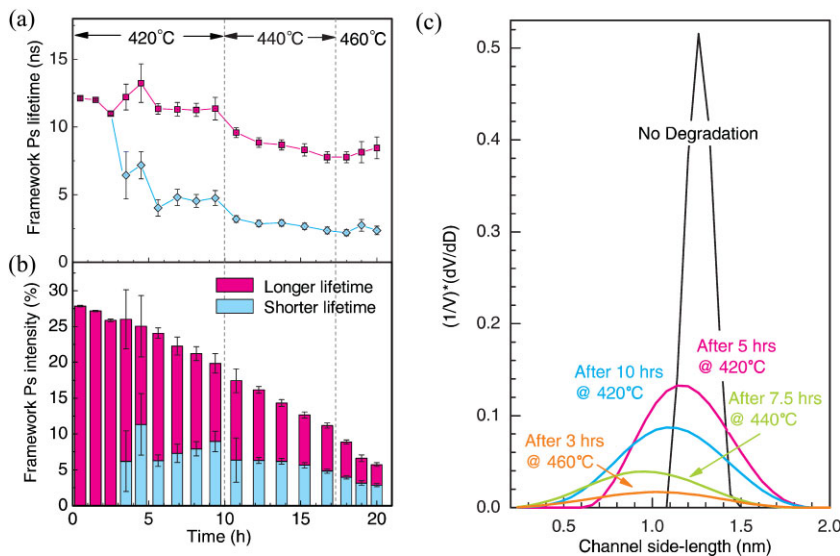


Figure 4. Monitoring thermal degradation. a) Irreversible changes in the lifetimes and b) corresponding relative intensities for Ps probing the MOF-5 framework above 400 °C. c) Room-temperature pore-size distributions (fractional free volume in long, square-channeled pores in the side-length range D to $D + \Delta D$) acquired at various intervals of heat treatment. The area under each curve has been normalized to the total Ps intensity (from Fig. 4b) and serves as a relative measure of total porosity.

PALS provides a new way of viewing the porous volume of MCPs that is highly complementary to the traditional probes. The nominal cage size is readily extracted from the framework Ps lifetime and, in the particular case of MOF-5, a long Ps lifetime indicates the discovery of much larger, 6-nm defects that comprise $\sim 0.02\%$ porosity. The Ps diffusion length within the framework is related to the cage aperture and, ultimately, the guest mobility. The most attractive feature of PALS is the ability to characterize MCPs in situ during exposure to gases and extreme temperatures that can affect the framework structure, its filling (or conspicuous lack thereof to reveal potentially functional residual porosity), or framework damage evolution and collapse. Continuously monitoring pore structure parameters is considerably more informative than simple post-processing characterization. Several additional outstanding issues in MCPs that can be illuminated by application of PALS include structural interpenetration, framework flexibility, and multiple-gas adsorption. These studies are underway.

Experimental

Synthesis of MCPs: MOF-5 [28] and zinc 2-methylimidazole [19] were synthesized as previously described.

PALS: The MCP was loaded in a high-purity N_2 glove box into a variable-pressure cell containing a 10 mCi ^{22}Na positron source sealed between thin kapton sheets. These energetic beta decay positrons penetrate through the kapton sheets and implant ~ 0.2 mm into the MCP, hence probing the bulk of the crystals. A separate source sealed with 5- μ m-thick Ni foil was used in the heating experiments. The sample is evacuated to 10^{-2} Torr so that Ps would not form or interact with any residual gas. The methodology and results for depth-profiled PALS using a monoenergetic positron beam in vacuum are discussed in the Supporting Information.

Acknowledgements

This work is supported by the National Science Foundation (DMR-0907369). Supporting Information is available online from Wiley InterScience or from the author.

Received: October 21, 2009
Published online: January 7, 2010

- [1] H. K. Chae, D. Y. Siberio-Perez, J. Kim, Y. Go, M. Eddaoudi, A. J. Matzger, M. O'Keefe, O. M. Yaghi, *Nature* **2004**, 427, 523.
- [2] G. Férey, C. Mellot-Draznieks, C. Serre, F. Millange, J. Dutour, S. Surble, I. Margiolaki, *Science* **2005**, 309, 2040.
- [3] K. Koh, A. G. Wong-Foy, A. J. Matzger, *Angew. Chem. Int. Ed.* **2008**, 47, 677.
- [4] Y. Yan, X. Lin, S. H. Yang, A. J. Blake, A. Dailly, N. R. Champness, P. Hubberstey, M. Schroder, *Chem. Commun.* **2009**, 1025.
- [5] K. Koh, A. G. Wong-Foy, A. J. Matzger, *J. Am. Chem. Soc.* **2009**, 131, 4184.
- [6] K. M. Thomas, *Dalton Trans.* **2009**, 1487.
- [7] G. Férey, *Chem. Soc. Rev.* **2008**, 37, 191.
- [8] D. Maspoth, D. Ruiz-Molina, J. Veciana, *Chem. Soc. Rev.* **2007**, 36, 770.
- [9] S. Kitagawa, R. Kitaura, S. Noro, *Angew. Chem. Int. Ed.* **2004**, 43, 2334.
- [10] A. G. Wong-Foy, A. J. Matzger, O. M. Yaghi, *J. Am. Chem. Soc.* **2006**, 128, 3494.
- [11] S. R. Caskey, A. G. Wong-Foy, A. J. Matzger, *J. Am. Chem. Soc.* **2008**, 130, 10870.
- [12] P. L. Llewellyn, S. Bourrelly, C. Serre, A. Vimont, M. Daturi, L. Hamon, G. De Weireld, J. S. Chang, D. Y. Hong, Y. K. Hwang, S. H. Jung, G. Férey, *Langmuir* **2008**, 24, 7245.
- [13] D. W. Gidley, H. G. Peng, R. S. Vallery, *Ann. Rev. Mater. Res.* **2006**, 36, 49.
- [14] M. Eldrup, D. Lightbody, J. N. Sherwood, *Chem. Phys.* **1981**, 63, 51.
- [15] S. J. Tao, *J. Chem. Phys.* **1972**, 56, 5499.
- [16] T. L. Dull, W. E. Frieze, D. W. Gidley, J. N. Sun, A. F. Yee, *J. Phys. Chem. B* **2001**, 105, 4657.
- [17] B. Jasinska, A. L. Dawidowicz, T. Goworek, J. Wawryszczuk, *Opt. Appl.* **2002**, 7.
- [18] H. Li, M. Eddaoudi, M. O'Keefe, O. M. Yaghi, *Nature* **1999**, 402, 276.
- [19] X. C. Huang, Y. Y. Lin, J. P. Zhang, X. M. Chen, *Angew. Chem. Int. Ed.* **2006**, 45, 1557.
- [20] Although the 3D model is not appropriate for the vacant MOF we retain it here as we will present evidence that Ps diffusion is strongly curtailed at CO_2 saturation adsorption and may then be localized in 3D.
- [21] A. R. Millward, O. M. Yaghi, *J. Am. Chem. Soc.* **2005**, 127, 17998.
- [22] S. Hermes, M. K. Schroter, R. Schmid, L. Khodeir, M. Muhler, A. Tissler, R. W. Fischer, R. A. Fischer, *Angew. Chem. Int. Ed.* **2005**, 44, 6237.
- [23] D. Esken, X. Zhang, O. I. Lebedev, F. Schroder, R. A. Fischer, *J. Mater. Chem.* **2009**, 19, 1314.
- [24] S. S. Han, J. L. Mendoza-Cortes, W. A. Goddard, *Chem. Soc. Rev.* **2009**, 38, 1460.
- [25] F. Salles, A. Ghoufi, G. Maurin, R. G. Bell, C. Mellot-Draznieks, G. Férey, *Angew. Chem. Int. Ed.* **2008**, 47, 8487.
- [26] G. L. Wright, M. Charlton, G. Clark, T. C. Griffith, G. R. Heyland, *J. Phys. B: At. Mol. Opt. Phys.* **1983**, 16, 4065.
- [27] D. W. Gidley, W. E. Frieze, T. L. Dull, J. Sun, A. F. Yee, C. V. Nguyen, D. Y. Yoon, *Appl. Phys. Lett.* **2000**, 76, 1282.
- [28] M. Eddaoudi, J. Kim, N. Rosi, D. Vodak, J. Wachter, M. O'Keefe, O. M. Yaghi, *Science* **2002**, 295, 469.